Published in Physical Review A 82, 063810, 1-7, 2010
which should be used for any reference to this work

Light effects in the atomic-motion-induced Ramsey narrowing of dark resonances in wall-coated cells

E. Breschi,[1] G. Kazakov,[2] C. Schori,[1] G. Di Domenico,[1] G. Mileti,[1] A. Litvinov,[2] and B. Matisov[2]
[1]*Laboratoire Temps-Fréquence–University of Neuchâtel, CH-2000 Neuchâtel, Switzerland*
[2]*St. Petersburg State Polytechnic University, RU-195251 St. Petersburg, Russia*

We report on light shift and broadening in the atomic-motion-induced Ramsey narrowing of dark resonances prepared in alkali-metal vapors contained in wall-coated cells without buffer gas. The atomic-motion-induced Ramsey narrowing is due to the free motion of the polarized atomic spins in and out of the optical interaction region before spin relaxation. As a consequence of this effect, we observe a narrowing of the dark resonance linewidth as well as a reduction of the ground states' light shift when the volume of the interaction region decreases at constant optical intensity. The results can be intuitively interpreted as a dilution of the intensity effect similar to a pulsed interrogation due to the atomic motion. Finally the influence of this effect on the performance of compact atomic clocks is discussed.

I. INTRODUCTION

Since the development of antirelaxation wall coatings in the 1950s [1] this technology has been used to increase the coherence time of atoms confined in vapor cells. With a coating material such as paraffin the atomic coherence can survive several thousand wall collisions leading to observed linewidths of only a few hertz on either Zeeman [2,3] or hyperfine transitions [4]. These narrow linewidths allowed an increase in the sensitivity of atomic magnetometers [5] and the short-term stability of atomic clocks [6]. In recent years there has been considerable progress in miniaturizing magnetometers and frequency standards using microfabricated vapor cells [7]. However, the reduced volume-to-surface ratio in a small vapor cell increases the wall collision rate and limits the device performance. This limitation has lead to a renewed interest in coating technology [8,9] and effects related to spectroscopy in wall-coated cells [10].

In this article, we address a particular narrowing of transit-time-broadened resonances due to atomic motion that is explained in analogy to Ramsey spectroscopy. In Ramsey spectroscopy [11] the ensemble of quantum systems (atoms or molecules) is interrogated by a series (at least two) of coherent electromagnetic fields separated in time. The Ramsey interrogation can be realized either with an atomic (or molecular) beam propagating through two spatially separated fields, or with a pulsed electromagnetic field ([12] and references therein). Atomic-motion-induced Ramsey narrowing has been, recently, observed by Xiao *et al.* [13,14] in the case of the coherent population trapping (CPT) effect [15–17] studied in buffer gas cells. The signature of this effect is the spectral narrowing of the dark resonances due to diffusion of oriented atomic spins in and out of the optical interaction region. In Ref. [14], the authors develop a model based on integrating the rate equations for the possible Ramsey sequences weighted by their probability to occur. The calculation of this probability is based on the diffusion mode symmetry of alkalis diffusing in a buffer gas [18]. The effects of diffusion transport of excited or coherent atoms in buffer gas cells were also investigated theoretically and experimentally in Refs. [19,20]. Finally the CPT effect in the pulsed interrogation regime has been studied by Zanon *et al.* [21] and by Failache *et al.* [22], and in both cases a strong light-shift reduction and a narrowing of the dark resonance is demonstrated.

In wall-coated alkali-metal vapor cells without buffer gas, the atoms move randomly in the cell from wall to wall with constant velocity and direction. If the interrogation volume is smaller than the cell volume the atom interacts with a pulsed electromagnetic field whose pulse duration depends on the velocity and trajectory of the atom itself. In the case of a buffer gas cell only a part of the atoms diffuse out of the beam, while in a wall-coated cell, the atoms make many passages through the laser beam. We study the atomic-motion-induced Ramsey narrowing of dark resonances prepared in a wall-coated cell without buffer gas. In particular we characterize the light shift and narrowing of the clock resonance. We observe that both the linewidth and the light-shift coefficient decrease with the volume of the interaction region at fixed optical intensity. This behavior is explained qualitatively by noting that the time an atom spends in the interaction region is proportional to the volume of this region. A three-level model is used to fit the experimental data; despite its simplicity this approach points out the scaling with interaction volume and optical intensity.

This article is organized as follows: we introduce the experimental apparatus (Sec. II) and the main observations (Sec. III); then, in Sec. IV, we discuss the phenomenological interpretation of the results and the relevance for application to compact atomic clocks.

II. EXPERIMENTAL APPARATUS

We performed our experiments with a conventional dark-line spectroscopy method. The signal is due to the hyperfine (hf) CPT prepared with linearly polarized laser light (the so-called lin∥lin CPT) [23]. This light-atom configuration is particularly interesting for the D_1 manifold of alkali-metal atoms because in this configuration there is an enhancement of the CPT strength due to the absence of spectator states when the excited state involved in the transitions has the lowest F_e. We discussed this light-atom interaction configuration in detail

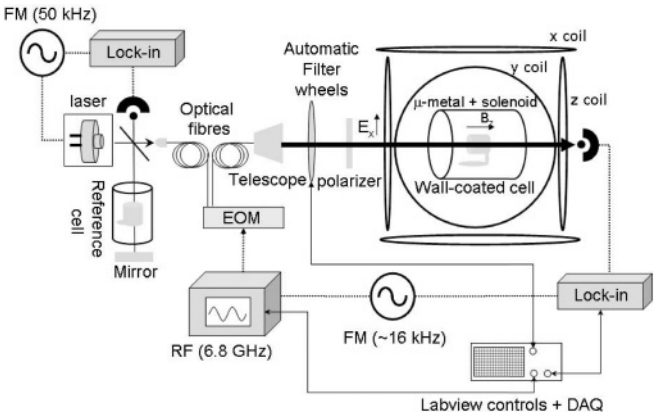

FIG. 1. Scheme of the experimental apparatus. The light emitted by a distributed feedback (DFB) diode laser is separated in two parts. One part is used for optical frequency stabilization based on the saturated absorption signal in an evacuated uncoated reference cell. The second part is used for the main experiment: it is modulated by an electo-optical (EOM) at $\nu_{\rm hf} = 6.834\,682\,610$ GHz and collected on a photodetector after passing through the different optic elements and the wall-coated cell.

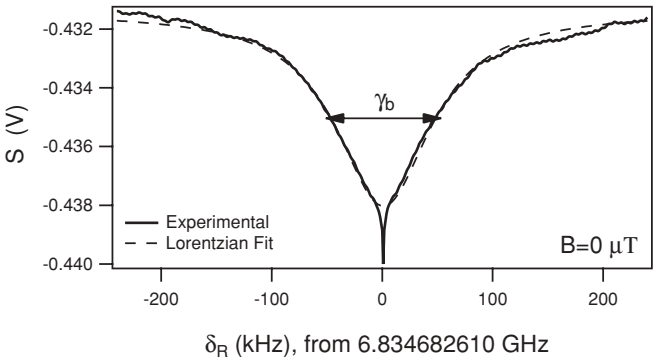

FIG. 2. Measurement of the typical dual structure [29] of dark resonances prepared in wall-coated cells. The resonant laser power is 12.1 μW and the laser beam radius is 1.5 mm (corresponding to a resonant laser intensity of 0.17 mW cm^{-2}). δ_R is the two-photon Raman detuning. The signal is recorded at zero magnetic field to avoid magnetic broadening and lineshape deformation of the broad resonance. The broad resonance has a linewidth (full width at half maximum (γ_b) of the Lorentzian fit) of about 100 kHz mainly determined by transit time and intensity broadening [33]. The linewidth of the narrow resonance is about 1000 times narrower than the linewidth of the broad resonance.

in Ref. [24] for the case of ^{87}Rb atoms contained in a buffer gas cell. The experimental apparatus is sketched is Fig. 1. We use a cylindrical cell which has the external diameter and length both equal to 14 mm and is filled with isotopically enriched ^{87}Rb (hyperfine separation $\nu_{\rm hf} = 6.834\,682\,610$ GHz). The internal walls of the cell are coated with Paraflint, a commercial paraffin well known for its particularly good antirelaxation properties [25,26]. We monitor the light transmitted through the cell when the detuning between two resonant frequencies in the laser spectrum (i.e., the Raman detuning δ_R) is swept around $\nu_{\rm hf}$. The cell temperature is stabilized at 57°C whereas the atomic reservoir temperature is 55°C to avoid deposition of Rb metal on the cell windows. The laser source used in the experiments is a distributed feedback (DFB) diode laser emitting at 795 nm, i.e., resonant with the D_1 line of ^{87}Rb [27]. The output beam of the DFB is modulated at $\nu_{\rm hf}$ by an electro-optical modulator (EOM). The phase modulation index (M) is about 1.5 and it has been measured with a Fabry-Perot interferometer. For this value of M, about 90% of the total laser power is equally distributed in the carrier and the first-order sidebands. The light transmitted by the EOM passes a telescope for varying the laser diameter in the range $(1,\ldots,8)$ mm, a filter to vary the optical intensity, a polarizer to control the laser polarization (E_y), the wall-coated cell, and, finally, it is collected on a photodetector. The laser is stabilized using a separate evacuated and uncoated cell on the Doppler-free peak (transition $|F_g = 2\rangle \rightarrow |F_e = 1\rangle$). The wall-coated cell is centered inside a μ-metal cylinder and the residual field is compensated using three orthogonal pairs of coils in Helmholtz configuration. A dc magnetic field ($B_z = 0.4\,\mu$T) is applied parallel to the laser beam propagation vector by means of a solenoid mounted inside the μ-metal cylinder. The signal transmitted through the cell is monitored with a digital oscilloscope and a lock-in amplifier. Particular attention has been devoted to the measure of the laser beam radius, since it is the relevant parameter for our study. We measure the laser beam diameter at $1/e^2$ (13.5%) of the peak intensity with a Thorlabs beam profiler (BP109-IR) in the two directions perpendicular to the laser propagation. The laser intensity distribution follows a Gaussian profile with the same characteristic in both directions.

III. EXPERIMENTAL RESULTS

A. Atomic-motion-induced Ramsey narrowing of transit time broadening

Figure 2 represents the typical dual-structure of the dark resonance prepared in a wall-coated cell. This dual structure, which has also been observed in nonlinear Faraday-effect spectra [28], is due to the atomic-motion-induced Ramsey narrowing of the transit-time-broadened resonance [29]. The signal is recorded at zero magnetic field in order to avoid magnetic broadening and lineshape deformation of the broad resonance. Note that in our experiments the residual Doppler effect is reduced by the Dicke narrowing because the atoms are confined in a cell with a characteristic length smaller than the wavelength of 4.4 cm corresponding to $\nu_{\rm hf}$ [30–32]. A detailed review of different coherence relaxation effects has been recently published by Xiao in Ref. [33]. The broad-resonance linewidth (γ_b) is about 100 kHz and is mainly limited by one time crossing of atoms with the interaction volume. Thus γ_b can be interpreted in analogy with the case of dark resonance prepared in an evacuated uncoated cell: $\gamma_b \approx \Gamma_t + \Gamma_I$, where $\Gamma_t \approx 30$ kHz is the transit time contribution [34] and the term Γ_I is the intensity broadening contribution [35]. In contrast, the narrow resonance is a factor of 1000 narrower than broad resonance as a consequence of the atomic-motion-induced Ramsey narrowing due to atoms passing several times through the beam before decoherence.

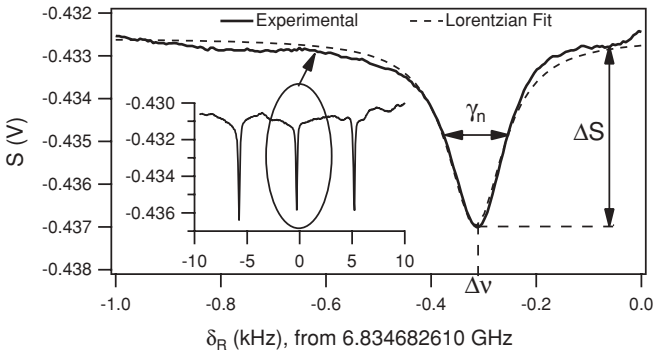

FIG. 3. Measurement of the narrow resonance corresponding to Fig. 2 when a longitudinal magnetic field $B_z = 0.4$ μT is applied to remove the Zeeman degeneracy. The Zeeman structure of the CPT spectrum is shown in the inset. We focus our attention on the magnetic-insensitive dark resonance used in clock applications. The resonance linewidth (γ_n), amplitude (ΔS), and frequency shift ($\Delta\nu$) are 130 Hz, 4 mV, and -316 Hz, respectively.

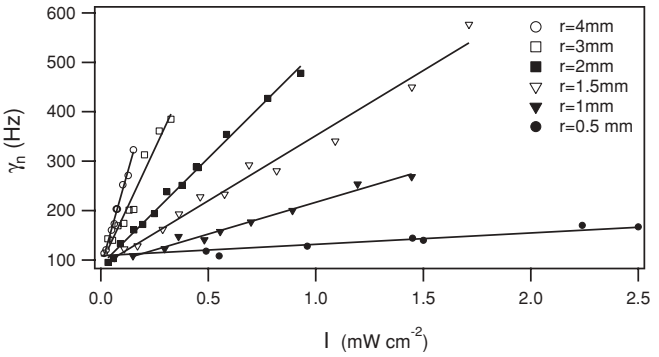

FIG. 4. Measurement of the linewidth (γ_n) of the dark resonance as a function of the laser intensity contained in the carrier and one of the first-order sideband incidents on the cell, that is, the resonant laser intensity (I). The laser beam radius (r) is varied from 0.5 to 4 mm. The points are the experimental values while the lines are the linear fits with Eq. (1).

B. Effect of the interaction volume on light shift and broadening of the dark resonance

In this section we focus our attention on light effects in the atomic-motion-induced Ramsey narrowing. More precisely, we use CPT spectroscopy to measure the light-induced broadening and the light shift of the magnetic-insensitive dark resonance used in clock applications. Figure 3 represents a zoom of the central part of Fig. 2 when a longitudinal magnetic field of 4 μT is applied to remove the Zeeman degeneracy of the narrow resonance. In the inset of Fig. 3 the complete Zeeman structure of the CPT spectrum is shown. We study the linewidth (γ_n), the amplitude (ΔS), and the frequency shift ($\Delta\nu$) from the unperturbed hyperfine frequency of the narrow resonance as a function of the resonant laser intensity (I) and of the laser beam radius (r). For the data interpretation we assume that the dark resonances have Lorentzian lineshape as predicted by a model describing a symmetric three-level atom at rest in the case of resonant, low-intensity light fields [35]. A detailed analysis of the lineshape modification due to the atomic-motion-induced Ramsey narrowing requires a more complete model accounting for the characteristic of both the atomic system and the laser light, as well as the motion-induced Ramsey sequences. Nevertheless, the phenomenological approach used here allows one to understand the main features of the phenomenon and thus predict how the linewidth and frequency shift scale with the interaction volume.

1. Light-induced broadening of the dark resonance

We measured the dark resonance as a function of the laser intensity and for different values of the laser beam radius. Then, we obtained the linewidth γ_n from a Lorentzian fit of the dark resonance, as shown in Fig. 3, and the results are reported in Fig. 4. We observe that the optical field induces a broadening of the narrow resonance which is proportional to the intensity I. Moreover, the linewidth γ_n is less sensitive to intensity changes for small beam diameter similarly to the results presented in Refs. [13,21]. Following the model presented in Ref. [35] the linewidth of the dark resonance can be written as

$$\gamma_n = \Gamma + gI, \tag{1}$$

where Γ is proportional to the relaxation rate of the ground-state coherence and g is the light broadening coefficient which depends on the characteristics of the atomic transitions being excited. The lines in Fig. 4 were obtained by fitting Eq. (1) to our experimental data.

In the case of an atomic system contained in an evacuated wall-coated cell, Γ is limited by the atom-wall coating collisions [25,36], the spin-exchange collisions [37], and the contribution from the atoms escaping through the Rb reservoir [26]. We evaluated the contribution of the spin-exchange and the reservoir losses to be of the order of a few tens of hertz and a few hertz, respectively. Therefore, the most relevant contribution to Γ comes from the collisions between the Rb atoms and the coating. This last contribution depends on the cell geometry but does not depend on the radius r of the optical interaction region. In contrast, the light-induced broadening of the linewidth does depend on r and is therefore modified by the motion-induced Ramsey narrowing. In Fig. 5 one can observe the proportionality between the light broadening coefficient (g) corresponding to the data reported in Fig. 4 and the square of the laser beam radius (r^2).

In summary, we observe a narrowing of the resonance linewidth when the volume of the optical interaction region decreases at constant optical intensity. For comparison, in an evacuated uncoated cell the linewidth increases when the volume of the interaction region decreases; that is, the lower limit of the linewidth is achieved when the whole cell volume is illuminated [38].

2. Light shift of the dark resonance

In Fig. 3 one can observe that the experimental resonance frequency is shifted from the unperturbed value by $\Delta\nu = -316$ Hz. For our experimental condition this shift is mainly due to collisions with the coated wall. The coating shift is negative and in qualitative agreement with previous results [25]. Furthermore we have measured the spectral position of

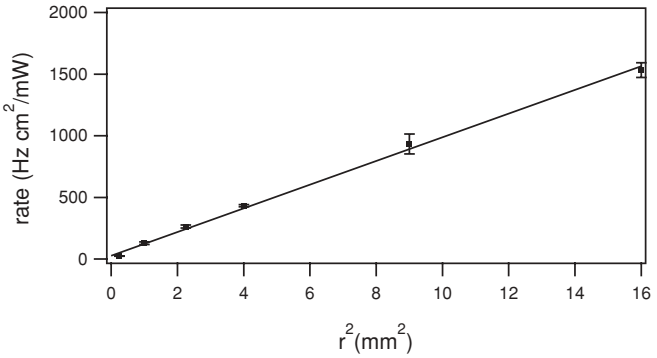

FIG. 5. Evolution of the light broadening coefficient g as a function of the square of the laser beam radius r^2. The values of g were obtained by fitting Eq. (1) to the data of Fig. 4.

the absorption minimum of the dark resonance as a function of light intensity for different values of r. These frequency shifts are referred to as light shift [39] and they depend on the characteristics of the interrogating light fields (intensity, polarization, one-photon laser detuning, and spectral distribution). These shifts can set the limit of the medium-term and long-term stability performance of CPT-based atomic clocks via the instability of the laser intensity and frequency. In modulated CPT clocks, both the resonant and the off-resonant optical sidebands contribute to light shifts. We observe that the dependence of resonance frequency shift on intensity is approximately linear [40] and determine the light-shift coefficient (LS) as the slope of the normalized frequency shift $(\Delta\nu/\nu_{\rm hf})$ as a function of I. The light shift of the dark resonance can be qualitatively explained from the coupling to the non-resonant excited state hyperfine sublevel (which in our case is $F_e = 2$). In the lin$\|$lin configuration the light shift can be positive or negative depending on the electromagnetic field spectral distribution and on the one-photon optical detuning [41]. We have measured a negative light shift mainly due to the transitions $|F_g = 2, m_F = \pm 1\rangle \rightarrow |F_e = 2, m_F = 0\rangle$. In Fig. 6 the LS coefficient is represented as a function of the square of the laser beam radius r^2. The absolute value of the LS coefficient increases with r, as a consequence the shift $\Delta\nu$ is more sensitive to intensity fluctuations for larger interrogation volume.

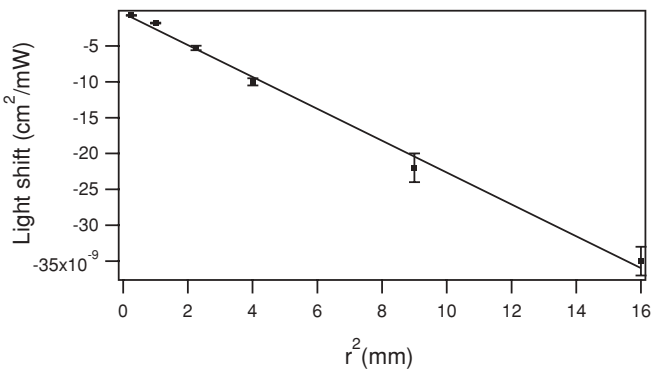

FIG. 6. Evolution of the light-shift coefficient (LS $= \partial y/\partial I$ with $y = \Delta\nu/\nu_{\rm hf}$) as a function of the square of the laser beam radius r^2.

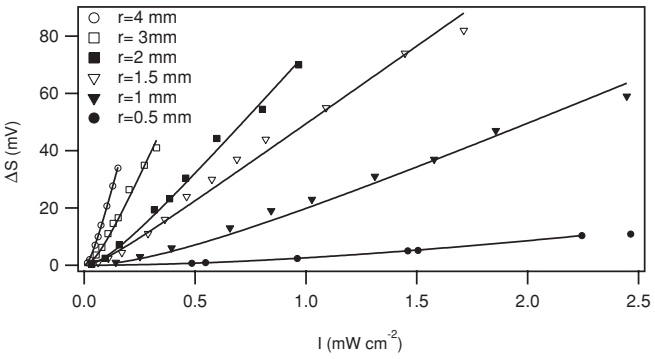

FIG. 7. Measurement of the dark resonance amplitude as a function of the laser intensity. The points are the experimental data, corresponding to the data reported in Fig. 4. Each line is a fit to the data using Eq. (2).

3. Dark resonance amplitude

We report in Fig. 7 the dark resonance amplitude ΔS as a function of the optical intensity for different values of the laser beam radius. The amplitude shows a quadratic dependence for intensities below the saturation value $I_s = \Gamma/g$, while the dependence is linear for intensities above this value. The value of the saturation intensity for each different beam radius is determined from the fit in Fig. 4. We use the obtained value of I_s to fit (solid curves in Fig. 7) the resonance amplitude with the expression derived in Ref. [35]:

$$\Delta S = n\frac{(I/I_s)^2}{1 + I/I_s}, \tag{2}$$

where n, the only free-scale parameter of the fit, is proportional to the density of rubidium atoms. In the linear regime the amplitude therefore scales as (I/I_s), which is proportional to the rate g shown in Fig. 5 and scales with r^2. The increase in resonance amplitude with laser beam radius can be explained qualitatively as an increase in the number of interacting atoms in the interrogation volume.

IV. DISCUSSION OF THE RESULTS

A. Phenomenological interpretation

The movement of an atom inside a cylindrical cell partially illuminated with a laser beam is represented in Fig. 8. We assume that the spatial distribution of the laser intensity is homogeneous. In this simplified picture the cell volume is essentially divided into one *bright* zone, that is, the cylinder illuminated by the laser beam (in gray in Fig. 8) and one *dark* zone outside the cylinder illuminated by the laser beam. When the laser beam radius (r) is smaller than the cell radius (R), the atom goes in and out of the bright zone. As a consequence, its interaction with the optical field is a time sequence of pulses, and on average the atom will spend a fraction r^2/R^2 of its time in the bright zone.

At low intensity, the finite interaction time during a single passage through the bright zone limits the linewidth γ_b, the same as observed in an uncoated cell. In contrast, in a wall-coated cell, this interaction time increases and γ_n is determined by the ground-state decoherence induced by the wall-coating collisions plus the light-induced broadening Γ_I. In the specific

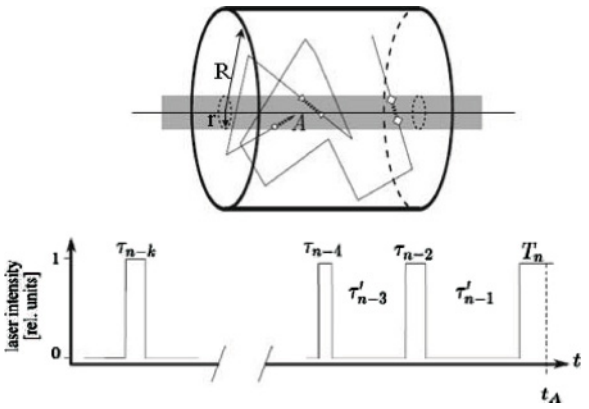

FIG. 8. Sketch of the vapor cell used to explain the dynamics of the light-atom interaction. The trajectory of the atom is represented by a dotted (solid) line when the atom moves inside (outside) the laser beam. The $[t, I]$ plot summarizes the interaction sequence for a generic atom, where I is the normalized laser intensity and t is the time. The atomic spin evolves freely when $I = 0$ while the atom interacts with the laser for $I \neq 0$, and after the time t_A the atom is detected. The interaction time for each passage in our experiments is of the order of 10 μs.

case of the narrow resonance, due to the dynamics of the interaction, Γ_I must be weighted by the fraction of time the atoms spend in the bright zone. Thus qualitatively the linewidth of the broad and narrow resonances can be derived as $\gamma_b = \Gamma + \Gamma_t + aI \approx \Gamma_t + aI$ and $\gamma_n = \Gamma + a\frac{r^2}{R^2}I$, respectively. For our experiment $\Gamma \approx 50$ Hz while Γ_t is tens of kHz: $\Gamma_t \approx \frac{\bar{v}}{2r}$, where $\bar{v} = 280$ m s^{-1} is the average atom velocity. In both cases a is a coefficient which depends on the atomic system. In summary for a fixed value of I, γ_b decreases while γ_n increases when we increase the value of r. A similar argument can be applied to the dark-resonance light shift which can be written as $\Delta\nu_{\rm LS} = \alpha\frac{r^2}{R^2}I$.

This simple phenomenological description explains the experimental observations reported in Sec. III B. However, a complete numerical model and simulations are required for a quantitative description of the Ramsey-like interaction sequences which depend on the geometry of the interaction and on the thermal motion of the atoms in the cell.

B. Impact on the performance of CPT-based atomic clocks

In this section we evaluate the impact of the wall-coated cell and the atomic-motion-induced Ramsey narrowing on the performance of a compact atomic clock based on the CPT effect.

As already mentioned in Sec. II, the lin$\|$lin configuration is studied for application in compact atomic clocks mainly because of the enhancement of the resonance contrast with respect to the σ^+ (or σ^-) configuration. In clock applications a high contrast is a crucial argument because the signal-to-noise ratio sets the limit for the short-term stability. However, when using linearly polarized laser light, the dark states prepared in the D_1 manifold are orthogonal; therefore, if simultaneously excited, they interfere destructively. The consequence of this quantum interference is the suppression of the CPT effect. In Ref. [24] we demonstrated that the quantum interference

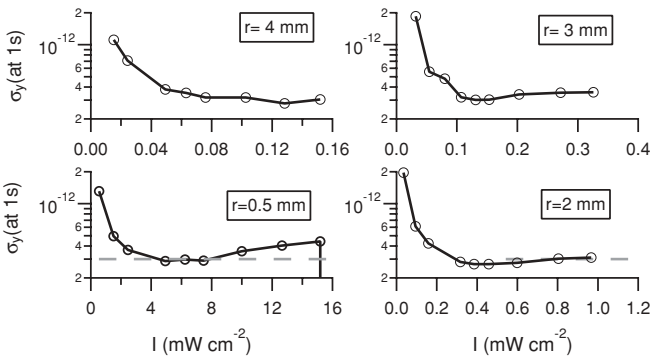

FIG. 9. Evolution of the Allan deviation $\sigma_y(1s)$ as a function of the laser intensity for different values of the laser beam radius. The values of $\sigma_y(1s)$ are calculated using Eq. (3) and the signal-to-(shot)noise measurements. In each plot the gray-dotted line corresponds to the value 3×10^{-13}, which is close to the optimal value obtained for each r.

depends on the pressure broadening of the optical transitions which does not occur in a wall-coated cell. Therefore, an advantage of using wall-coated cells instead of buffer gas cells is the possibility to obtain a better contrast of the dark resonance. Similar quantum interference effects have been discussed theoretically and in detail for the case of nonlinear magneto-optical rotation by Auzinsh and co-workers in Ref. [42].

If detection is shot-noise limited, the short-term stability of an atomic clock can be evaluated by the Allan deviation $\sigma_y(\tau)$ [43]:

$$\sigma_y(\tau) \propto \frac{k}{Q\Delta S/N_s}\tau^{-\frac{1}{2}}, \tag{3}$$

where k is a constant that depends on the type of modulation used for the phase-sensitive detection. ΔS is the signal amplitude, N_s is the shot noise, and Q is the resonance quality factor, that is, the ratio between the resonance frequency and the linewidth. In a typical clock experiment $k = 0.2$. However we chose $k = 1$ because we base our estimation on the dc signal and shot noise.

In the short-term limit ($\tau = 1$ s), N_s can be calculated from the photodetector current: $N_s = \sqrt{2eI_{\rm PD}}$, where e is the electron charge and $I_{\rm PD}$ is the photocurrent in the clock experimental conditions. Note that in N_s we account for the contribution of both the resonant part and the off-resonant part of the spectral distribution of the modulated laser. For practical reasons such as compactness and limited power consumption, a modulated diode laser is often preferred to other more bulky techniques that can provide light sources with higher spectral quality.

By using Eq. (3) we calculate the Allan deviation for different values of the laser intensity and of the laser beam radius. The values of $\sigma_y(1s)$ are reported in Fig. 9. These values are comparable with the performance predicted in a buffer gas cell with a laser source of higher spectral quality (two phase-locked extended cavity diode lasers [44]). From Fig. 9 one can also see that for each value of r the optimal $\sigma_y(1s) \approx 3 \times 10^{-13}$ can be reached at different values of I.

Our measurements show that in a wall-coated cell the influence of the laser beam radius on the signal can be

compensated by adjusting the laser intensity. This can play an important role in the realization of a compact and high-performance atomic clock since it removes the need for optical elements dedicated to the manipulation of the laser beam diameter.

V. CONCLUSIONS

To summarize, we discuss the effect of the laser power and beam diameter on the CPT resonance observed in a wall-coated cell without buffer gas where atomic-motion-induced Ramsey narrowing takes place and plays an important role. In particular we study light-induced effects on the dark resonance prepared in the lin‖lin configuration which is a good candidate as a reference for vapor cell atomic clocks.

We demonstrate that the atomic motion in and out of the interaction region reduces the effect of light intensity. Specifically, we observe a narrowing of the dark resonance and a reduction of the light shift when the optical interrogation volume is decreased. We propose an intuitive explanation of the dependence of the linewidth, amplitude, and light shift of the dark resonance on the laser beam radius (which determines the volume of the optical interrogation region). The atomic-motion-induced Ramsey narrowing can play a relevant role when only a part of the cell volume is illuminated even for coating materials (such as OTS [8]) having antirelaxation properties worse than those of the Paraflint.

Finally we discuss the relevance of the results for the application in compact and high-performance atomic clocks. The excitation of the lin‖lin CPT effect in a wall-coated cell is very promising in terms of short-term stability. Based on our signal-to-(shot)noise measurements we estimate that a $\sigma_y(1s) \approx 3 \times 10^{-13}$ can be obtained even with a small laser beam diameter.

ACKNOWLEDGMENTS

We are grateful to Professor Pierre Thomann for the stimulating discussion. This work was supported by the Swiss National Foundation (Project No. 200020-105624); the Association Suisse de la Recherche Horlogére (ASRH); the Russian Federal Special-Purpose Program “Science and Science-Pedagogical Personnel of Innovation Russia 2009–2013” (Contract No. П 2326); Grant No. RFBR -09-02-90465_ Ukr_ f_ a; and a grant of the President of Russian Federation for young postdocs, Project MK-5318.2010.2.

[1] H. G. Robinson, E. S. Ensberg, and H. G. Dehmelt, Bull. Am. Phys. Soc. **3**, 9 (1958).
[2] D. Budker, V. Yashchuk, and M. Zolotorev, Phys. Rev. Lett. **81**, 5788 (1998).
[3] D. Budker, W. Gawlik, D. F. Kimball, S. M. Rochester, V. V. Yashchuk, and A. Weis, Rev. Mod. Phys. **74**, 1153 (2002).
[4] H. G. Robinson and C. E. Johnson, Appl. Phys. Lett. **40**, 771 (1982).
[5] S. Groeger, G. Bison, J.-L. Schenker, R. Wynands, and A. Weis, Eur. Phys. J. D **38**, 239 (2006).
[6] A. Risley, S. Jarvis, and J. Vanier, J. Appl. Phys. **51**, 4571 (1980).
[7] S. Knappe, *MEMS Atomic Clocks* (Elsevier, Amsterdam, 2009), pp. 572–605.
[8] Y. W. Yi, H. G. Robinson, S. Knappe, J. Maclennan, C. D. Jones, C. Zhu, N. A. Clark, and J. Kitching, J. Appl. Phys. **104**, 023534 (2008).
[9] M. Balabas, T. Karaulanov, M. Ledbetter, and D. Budker, Phys. Rev. Lett. **105**, 070801 (2010).
[10] W. Wasilewski, K. Jensen, H. Krauter, J. J. Renema, M. V. Balabas, and E. S. Polzik, Phys. Rev. Lett. **104**, 133601 (2010).
[11] N. F. Ramsey, Phys. Rev. **78**, 695 (1950).
[12] F. Riehle, *Frequency Standards: Basics and Applications* (Wiley-VCH, New York/Weinheim, 2004).
[13] Y. Xiao, I. Novikova, D. F. Phillips, and R. L. Walsworth, Phys. Rev. Lett. **96**, 043601 (2006).
[14] Y. Xiao, I. Novikiva, D. F. Phillips, and R. L, Walsworth, Opt. Express **16**, 14128 (2008).
[15] K. Takagi, R. T. M. Su., and R. F. Curl, Appl. Phys. (Berlin) **7**, 298 (1975).
[16] G. Alzetta, A. Gozzini, L. Moi, and G. Orriolis., Nuovo Cimento B **36**, 5 (1976).
[17] E. Arimondo and G. Orriols, Lett. Nuovo Cimento Fis. **17**, 333 (1976).
[18] N. Beverini, P. Minguzzi, and F. Strumia, Phys. Rev. A **4**, 550 (1971).
[19] M. Gornyi and B. Matisov, Radiotech. Electron. **XXX**, 351 (1985) [in Russian].
[20] Z. D. Grujić, M. M. Mijailović, B. M. Panić, M. Minić, A. G. Kovacević, M. Obradović, B. M. Jelenković, and S. Cartaleva, Acta Phys. Pol. **112**, 799 (2007).
[21] T. Zanon, S. Guerandel, E. de Clercq, D. Holleville, N. Dimarcq, and A. Clairon, Phys. Rev. Lett. **94**, 193002 (2005).
[22] H. Failache, L. Lenci, and A. Lezama, Phys. Rev. A **81**, 023801 (2010).
[23] A. V. Taichenachev, V. I. Yudin, V. L. Velichansky, and S. A. Zibrov, Pis'ma ZhETF **82**, 449 (2005).
[24] E. Breschi, G. Kazakov, R. Lammegger, G. Mileti, B. Matisov, and L. Windholz, Phys. Rev. A **79**, 063837 (2009).
[25] J. Vanier and C. Audoin, *The Quantum Physics of Atomic Frequency Standards* (Hilger, Philadelphia, 1989).
[26] N. Castagna, G. Bison, G. Di Domenico, A. Hofer, P. Knowles, C. Macchione, H. Saudan, and A. Weis, Appl. Phys. B **96**, 763 (2009).
[27] D. A. Steck, Rubidium 87 D Line Data, Version 2.1.2, 2009.
[28] S. I. Kanorsky, A. Weis, and J. Skalla, Appl. Phys. B **60**, S165 (1995).
[29] M. Klein, I. Novikova, D. F. Phillips, and R. L. Walsworth, J. Mod. Opt. **53**, 2583 (2006).
[30] R. H. Dicke, Phys. Rev. **89**, 472 (1953).

[31] G. Kazakov, B. Matisov, A. Litvinov, and I. Mazets, J. Phys. B **40**, 3851 (2007).
[32] A. N. Litvinov, G. A. Kazakov, and B. G. Matisov, J. Phys. B **42**, 165402 (2009).
[33] Y. Xiao, Mod. Phys. Lett. B **23**, 661 (2009).
[34] J. E. Thomas and W. W. Quivers, Phys. Rev. A **22**, 2115 (1980).
[35] J. Vanier, A. Godone, and F. Levi, Phys. Rev. A **58**, 2345 (1998).
[36] M. A. Bouchiat and J. Brossel, Phys. Rev. **147**, 41 (1966).
[37] W. Happer, Rev. Mod. Phys. **44**, 169 (1972).
[38] F. Renzoni and E. Arimondo, Phys. Rev. A **58**, 4717 (1998).
[39] M. Arditi and T. R. Carver, Phys. Rev. **124**, 800 (1961).
[40] A. Nagel, S. Brandt, D. Meschede, and R. Wynands, Europhys. Lett. **48**, 385 (1999).
[41] S. A. Zibrov, I. Novikova, D. F. Phillips, R. L. Walsworth, A. S. Zibrov, V. L. Velichansky, A. V. Taichenachev, and V. I. Yudin, Phys. Rev. A **81**, 013833 (2010).
[42] M. Auzinsh, D. Budker, and S. M. Rochester, Phys. Rev. A **80**, 053406 (2009).
[43] J. Vanier and L. G. Bernier, IEEE Trans. Instrum. Meas. **IM-30**, 277 (1981).
[44] E. Breschi, G. Kazakov, R. Lammegger, G. Mileti, B. Matisov, and L. Windholtz, IEEE Trans. Ultrason. Ferroelectr. Freq. Control **56**, c5 (2009).